J M M
Journal of Mechanics and MEMS
Special Issue dedicated to Prof. K Y Ye edited by Z M Ye, P Liu and B Sun

ISSN: 0974-8407

9(2) 2017: pp. 391-399

MORPHOLOGY TRANSITION OF A LIQUID BRIDGE CONFINED BETWEEN TWO PARALLEL PLATES: AN AXISYMMETRICAL MODEL

Jianlin Liu*

ABSTRACT

A three-dimensional theoretical model is presented in the present paper to investigate the morphology transition of a liquid bridge confined between two chemically patterned plates. Depending upon the spacing between the two plates and the liquid volume, the liquid bridge may take several different morphologies, e.g., an out-bulging or an in-curved liquid bridge. We derive the phase diagram for the morphologies of a liquid bridge, allowing us to easily determine its shape under a specified condition. In addition, the force which the liquid bridge acts on the plates is derived. The obtained results might be helpful for a better understanding of some wetting phenomena associated with liquid bridges for industry to biology and can be used to estimate the influence of liquid bridge forces (or capillary forces) in microsized devices and systems.

***Keywords*:** liquid bridge, surface energy, superhydrophilic

1. INTRODUCTION

The wetting morphology of a liquid adsorbed on a solid substrate is related not only to the chemical compositions of the two phases [1] but also to the microstructures of the substrate [2]. By mimicking the fractal or hierarchical surface microstructures of plant leaves (e.g., lotus and the Lady's Mantle), some ultrahydrohpobic materials with contact angles larger than 160° have been fabricated successfully [3, 4]. In addition, geometrically smooth substrates with heterogeneous chemical nature also exhibit some interesting and unusual features of wetting. Liquid wetting phenomena on solid substrates with surface domains of various shapes (e.g., stripes, rings, circles, and micro-channels) have been investigated theoretically and experimentally [5~10]. Recently, for instance, Lipowsky and his coworkers [11] derived a stability criterion of a droplet on a substrate with surface domains of different shapes.

Another interesting issue is the analysis of liquid bridges constrained between two solid surfaces or between a solid and a liquid surface, which can be observed in various areas from engineering to biology. Considerable attention has been paid to the stability and morphology transition of liquid bridges/bubbles between two plates [12, 13], two spheres [14], an axisymmetric or spherical punch and a substrate [15]. Meseguer *et al.* [16] presented a review on the stability of liquid bridges between two solid disks and analyzed the non-axisymmetric effect as well as the influence of electric fields. Through investigation of liquid bridges, Obata *et al.* [17] suggested a novel scheme of micro-manipulation in MEMS, and Qian *et al.* [18] interpreted some phenomena of biological adhesion of such insects as beetles, blowflies and ants associated with capillary forces. Bock and Sacquin [19] investigated by Monte Carlo simulations the phase behavior of a fluid confined between two parallel solid substrate and considered the shear effect. Alencar *et al.* [20] analyzed the liquid bridge by Monte Carlo simulation of a lattice gas model and variational calculus based on minimization of the surface area with the volume and the contact angle constraints. Swain and Lipowsky [21], and Valencia *et al.* [22] analyzed the wetting morphology of a liquid bridge constrained between two plates with alternating hydrophilic and hydrophobic stripes. They adopted a two-dimensional plane model, which underestimated the influence of the surface tension of liquid.

* Department of Engineering Mechanics, China University of Petroleum, Qingdao 266555, China, *E-mail: jl-liu03@mails.tsinghua.edu.cn*

A more practical case is the three-dimensional liquid bridges between two solid surfaces. However, there is as yet a lack of three-dimensional investigation on the wetting morphology of liquid bridges because of its mathematical complexity. In the present paper, therefore, we formulated a three-dimensional model in terms of energy to study the morphological transition of liquid bridges constrained between two geometrically smooth but chemically patterned solid surfaces. The conditions of morphological transition among several representative morphologies are determined by the contact angle and contact radius of the liquid bridge. The phase diagram is given which allows us to determine the stable morphology of liquid bridge under given conditions. Finally, the liquid bridge force is derived through energy formulation when the shape of the liquid bridge changes.

2. THEORETICAL MODEL

Consider two identical parallel plates with chemically heterogeneous surface structure, each containing a circular hydrophilic one, *W*, of radius *r* and a hydrophobic one, *D*, as shown in Fig. 1. The centers of the two identically circular hydrophilic zones are coaxial. Let *H* denote the distance of the two plates. Refer to a Cartesian coordinate system (*o-xy*). If a liquid drop of volume *V* is constrained between the two hydrophilic zones, its shape will be axisymmetrical and it may bulge outward, curve inward or fracture apart (Figs. 1–3), depending on the parameters *r*, *V*, *H* and the Laplace pressure difference $\Delta p = p_v - p_L$, where p_V and p_L are the pressure of the vapor and the liquid, respectively. Here, we assume that the size of the liquid bridge is of microns and that the influences of line tension and gravity are negligible.

To determine the morphology transition of a liquid bridge from the viewpoint of energy, one needs to calculate its surface areas and volumes at different states. When Δp is negative, the liquid bridge will bulge out, as shown in Fig. 1. Its projection to the first quadrant of the *x-y* plane is approximated as an arc shape centered at $(x_0, H/2)$ and expressed as

$$(x - x_0)^2 + (y - H/2)^2 = R^2, \tag{1}$$

where $x_0 = r - \sqrt{R^2 - H^2/4}$, and *R* is the radius of the arc. The axisymmetric profile of the liquid bridge is obtained by rotating the arc of a circle with respect to the *y*-axis. The area of the liquid/vapor interface can be calculated from the following integral

$$S_1 = 2\int_r^{R+x_0} 2\pi x ds, \tag{2}$$

where $\mathrm{d}s = \sqrt{1 + y'^2}\,\mathrm{d}x$. Substituting Eq. (1) into (2), one has

$$S_1 = 4\pi R\int_r^{R+x_0} \frac{x}{\sqrt{R^2 - (x - x_0)^2}}\mathrm{d}x$$

$$= 4\pi R\left[\left(r - \sqrt{R^2 - \frac{H^2}{4}}\right)\arcsin\frac{H}{2R} + \frac{H}{2}\right]. \tag{3}$$

The volume of the liquid bridge is written as

$$V_1 = 2\pi\int_0^{H/2} x^2\mathrm{d}y \tag{4}$$

$$= \pi\left[Hr^2 + HR^2 - \frac{H^3}{12} - Hr\sqrt{R^2 - \frac{H^2}{4}} + 2R^2\left(r - \sqrt{R^2 - \frac{H^2}{4}}\right)\arcsin\frac{H}{2R}\right],$$

where $x = x_0 + \sqrt{R^2 - (y - H/2)^2}$.

When Δp is positive, the liquid bridge will curve inward, as shown in Fig. 2. Similar to the case of $\Delta p< 0$, the projection of the concave liquid drop to the first quadrant of the *x*-*y* plane is also an arc, which is expressed also by Eq. (1) but whose shape center abscissa x_0 is written as $x_0 = r + \sqrt{R^2 - H^2/4}$. The surface area of the liquid drop may be integrated as

$$S_2 = 4\pi R \int_{x_0 - R}^{r} \frac{x}{\sqrt{R^2 - (x - x_0)^2}} \mathrm{d}x \tag{5}$$

$$= 4\pi R \left[\left(r + \sqrt{R^2 - \frac{H^2}{4}} \right) \arcsin \frac{H}{2R} - \frac{H}{2} \right].$$

The volume of the liquid bridge is

$$V_2 = 2\pi \int_0^{H/2} \left[x_0^2 + R^2 - (y - H/2)^2 + 2x_0 \sqrt{R^2 - (y - H/2)^2} \right] \mathrm{d}y$$

$$= \pi \left[Hr^2 + HR^2 - \frac{H^3}{12} + Hr\sqrt{R^2 - \frac{H^2}{4}} - 2R^2 \left(r + \sqrt{R^2 - \frac{H^2}{4}} \right) \arcsin \frac{H}{2R} \right], \tag{6}$$

where $x = x_0 - \sqrt{R^2 - (y - H/2)^2}$.

3. DISCUSSIONS

With the increase in the spacing *H* of the two plates, the liquid bridge may lose its stability and be split into two droplets, both of which have the shape of spherical cap, as shown in Fig. 3.

For liquid bridges constrained between two solid plates, two situations have been considered in the literature, namely, the fixed volume ensemble and the fixed pressure difference ensemble. These two situations can be analyzed similarly, but in the present paper our attention is paid mainly to the former, which is of more practical interest.

Given a fixed volume of the liquid bridge, the dependence relationship of the radius *R* upon the spacing *H* can be calculated from Eq. (4) or (6). As the spacing *H* between the two plates varies, the liquid bridge may have several possible morphologies as follows (Fig. 4):

(A) an out-bulging liquid bridge with the contact line expanded into the *D* zone,

(B) an out-bulging liquid bridge with the contact line along the boundary of *W*,

(C) a circular cylinder with the contact line along the boundary of *W*,

(D) an in-curved liquid bridge with the contact line along the boundary of *W*,

(E) an in-curved liquid bridge with the contact line shrunk into the *W* zone,

(F) two liquid droplets formed as a result of liquid bridge breaking.

The six morphologies plotted in Fig. 4 occupy their own regions of stability. In what follows, we will give the conditions for the transitions of these different morphologies.

Firstly, when the contact line between the liquid bridge and the substrate is along the boundary of *W*, the contact angle is not constant but may vary in the range of $\theta_W \le \theta \le \theta_D$, where θ_W and θ_D are the contact angles of the hydrophilic (*W*) and hydrophobic (*D*) zones, respectively. From Fig. 1, the contact angle of an out-bulging liquid bridge can be expressed as

$$\theta = \pi - \arccos\left(\frac{1}{2} H/R \right). \tag{7}$$

As the separation H of the two plates decreases, the contact angle θ increases. The transition conditions between the morphologies A and B are

$$\theta = \theta_D \text{ and } a = r, \tag{8}$$

where a is the contact radius of the liquid bridge and the substrate. Without loss of any generality, it is assumed here that $\theta_W = 0$ and $\theta_D = \pi$. Combination of Eqs. (4) and (8) leads to the following equation for the boundary (curve 1) between the zones I and II in Fig. 4:

$$V_1' = \pi\left(Hr^2 + H^3/6 + \pi H^2 r/4\right). \tag{9}$$

With the further decrease of H when Eq. (8) has been satisfied, the contact line of the liquid will expand into the hydrophobic zone D.

Secondly, it is evident that the transition conditions between the morphologies B and D read

$$\theta = \frac{\pi}{2} \text{ and } a = r, \tag{10}$$

which corresponds to the morphology C, i.e., a circular liquid cylinder with the volume (the dashed line between the zones II and III in Fig. 4)

$$V_3' = \pi r^2 H. \tag{11}$$

Thirdly, for the in-curved liquid bridge with the contact line along the boundary of W (Fig. 2), the contact angle is variable in the range of $\theta_W \le \theta \le \pi i/2$. In this case, the contact angle can be expressed as

$$\theta = \arccos\left(\frac{1}{2}H/R\right). \tag{12}$$

Then the transition conditions between the morphologies D and E are

$$\theta = \theta_W \text{ and } a = r. \tag{13}$$

Substitution of Eq. (3) into (6) yields the following equation for the boundary (curve 3) between the zones II and III in Fig. 4:

$$V_2' = \pi\left(Hr^2 + H^3/6 - \pi H^2 r/4\right). \tag{14}$$

With the further increase of H when Eq. (15) has been satisfied, the contact line of the liquid will shrink into the hydrophobic zone W, that is, $a < r$.

Thus, for a given volume of the liquid, one can easily determine from Eqs. (9) and (14) its shape as a function of the spacing H of the two plates. In other words, one can give the respective ranges of H corresponding to an out-bulging (B) and an in-curved (D) liquid bridge. When $\tilde{V} = V/\left(\pi i^* r^3\right) = 1$, for example, the liquid bridge is out-bulging in the range of $0.638 \le \tilde{H} < 1$ and in-curved in the range of $1 < \tilde{H} \le 3.485$, where $\tilde{H} = H/r$. The morphologies A and E exist in the ranges $\tilde{H} < 0.638$ and $\tilde{H} < 3.485$, respectively. In addition, the dependence relationship of the curvature radius $\tilde{R} = R/r$ upon $\tilde{H} = H/r$ can also be obtained, as shown in Fig. 5. It is seen that with the increase of $\tilde{H}$, $\tilde{R}$ decreases for an out-bulging liquid bridge with $0.638 \le \tilde{H} < 1$ while it decreases first then increases for an in-curved liquid bridge with $1 < \tilde{H} \le 3.485$.

Fourth, in the process of the necking, when the thinnest part of the liquid bridge reduces to zero, it will break into two liquid droplets. The separating condition is

$$x_0 - R = r - R + \sqrt{R^2 - H^2/4} = 0 . \tag{15}$$

Substitution of Eq. (15) into (6) leads to critical volume of breaking of the liquid bridge

$$\tilde{V}_4 = \frac{V_4}{\pi r^3} = \frac{3\tilde{H}}{4} + \frac{\tilde{H}^3}{6} + \frac{\tilde{H}^5}{64} - \left(\frac{1}{2} + \frac{\tilde{H}^2}{8}\right)\left(\frac{1}{2} + \frac{\tilde{H}^2}{4} + \frac{\tilde{H}^4}{32}\right)\arcsin\frac{\tilde{H}}{1+\tilde{H}^2/4} . \tag{16}$$

Eq. (16) corresponds to the fracture curve 4 between the zones III and V in Fig. 4.

As a consequence of the morphology variation of the liquid bridge, an attractive or a repulsive force, which is referred to the capillary force or the liquid bridge force, will be exerted to the two plates. Much attention has been paid recently on liquid bridge forces because of their significant influence on the performance of micro- and nano-devices and systems, as well as on the measurements and experiments at small sizes [20]. Capillary forces play a significant role in the adhesion of surface micromechanical structures, e.g. hard-disk system [23]. The surface tension of the meniscus should also be considered in some AFM measurements. Belaubre *et al.* [24] uses a cantilever-based microsystem to produce DNA microarrays, where the the capillary force has great influence on the result. Johnstone *et al.* [25] made some theoretical analysis about the capillary force in cantilever measurement. In this section, the liquid bridge force in the configuration in Figs. 1–2 will be calculated from the viewpoint of energy. The liquid bridge force of some other configurations can also be calculated in the same manner, and the obtained solution can be used in explanation of some phenomena associated with capillary forces.

For example, we mainly consider the most representative cases of B, C and D in Fig. 4, where the boundary of the liquid bridge is identical to the interface between *W* and *D*. For the fixed volume ensemble, the free energy of the liquid bridge is expressed as [1]

$$U = \gamma S_{\mathrm{LV}} + \left(\gamma_{\mathrm{SL}} - \gamma_{\mathrm{SV}}\right) S_{\mathrm{SL}} , \tag{17}$$

where S_{LV} and S_{SL} denote the areas of the liquid/vapor and solid/liquid interfaces, respectively. S_{LV} is given in Section 2, and

$$S_{SL} = 2\pi r^2. \tag{18}$$

γ_{SL}, γ_{SL} and γ in Eq. (17) stand for the surface tensions of the solid/vapor, solid/liquid and liquid/vapor interfaces, respectively. They satisfy the Young's equation

$$\gamma_{SV} - \gamma_{SL} = \gamma \cos\theta_Y, \tag{19}$$

where θ_Y denotes the Young's contact angle of the liquid.

For example, as assumed above, the contact angle in the hydrophilic zone $\theta_Y = \theta_W = 0$, and then $\gamma_{SV} - \gamma_{SL} = \gamma$. Substituting Eqs. (18) and (19) into (17), the normalized free energy is expressed as

$$\tilde{U}_{\mathrm{i}} = U_{\mathrm{i}} / \left(\gamma\pi r^2\right) = \tilde{S}_{\mathrm{i}} - 2 , \tag{20}$$

where $\tilde{S}_{\mathrm{i}} = S_{\mathrm{i}} / \left(\pi r^2\right)$. The index *i* (*i* = 1, 2) corresponds to the two cases of out-bulging ($\Delta p < 0$) and inward-curving ($\Delta p > 0$), respectively.

The liquid bridge spanning will provide a force to the two plates. The force can be calculated from the derivation of the free energy of the system with respect to the height $\tilde{H}$ of the liquid bridge, i.e,

$$f_{\mathrm{i}} = -\frac{\mathrm{d}\tilde{U}_{\mathrm{i}}}{\mathrm{d}\tilde{H}} , \tag{21}$$

where the index i (*i* = 1, 2) corresponds to the two cases of out-bulging ($\Delta p < 0$) and inward-curving ($\Delta p > 0$), respectively.

For the considered ensemble of fixed volume, $\mathrm{d}\tilde{V}/\mathrm{d}\tilde{H} = 0$, where $\tilde{V} = \tilde{V}\left(\tilde{R}, \tilde{H}\right) = \tilde{V}\left(\tilde{R}\left(\tilde{H}\right), \tilde{H}\right)$. According to Eq. (4), therefore, one has

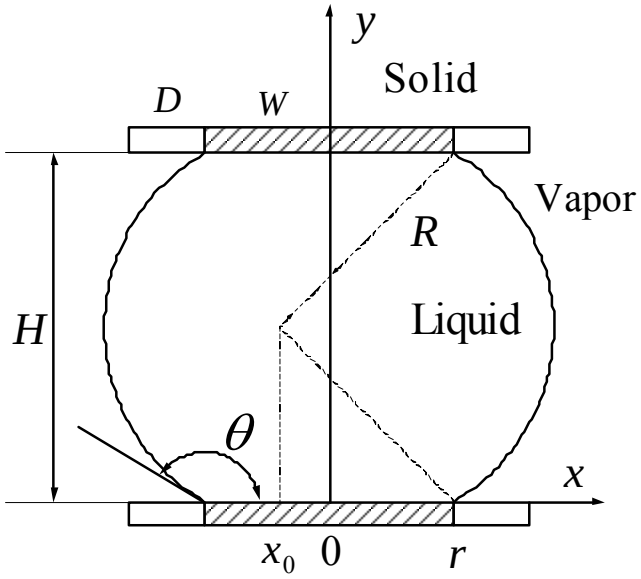

Figure 1: An Out-bulging Liquid Bridge Confined between Two Parallel Plates ($\Delta p < 0$)

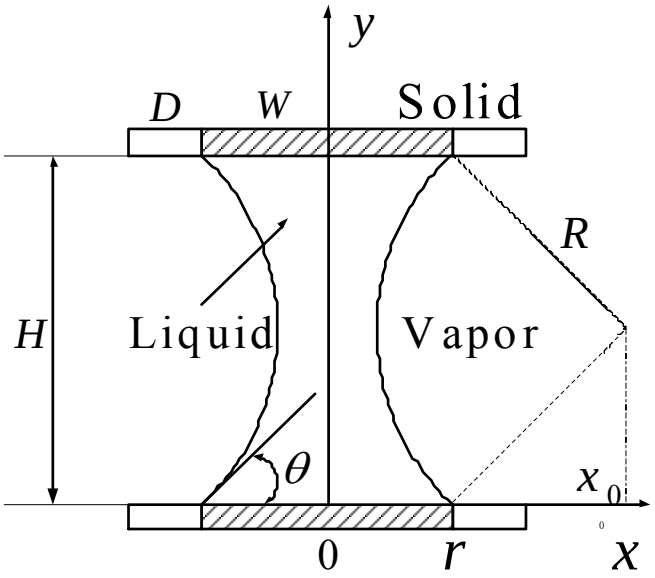

Figure 2: An In-curved Liquid Bridge Confined between Two Parallel Plates ($\Delta p > 0$)

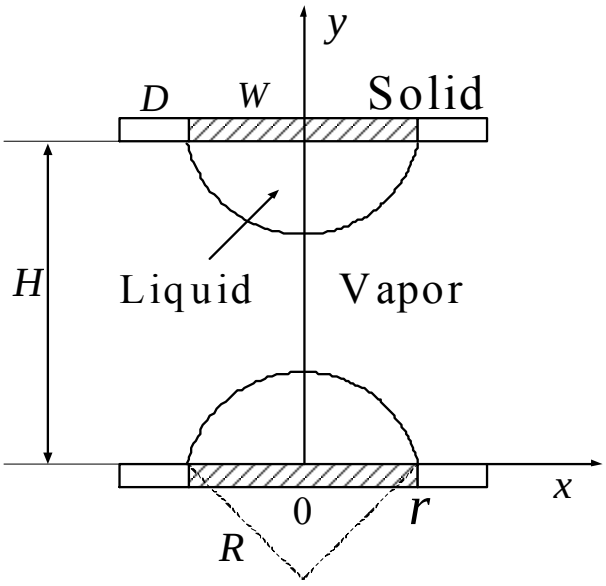

Figure 3: Two Identical Spherical Droplets Formed as a Result of Breaking of a Liquid Bridge

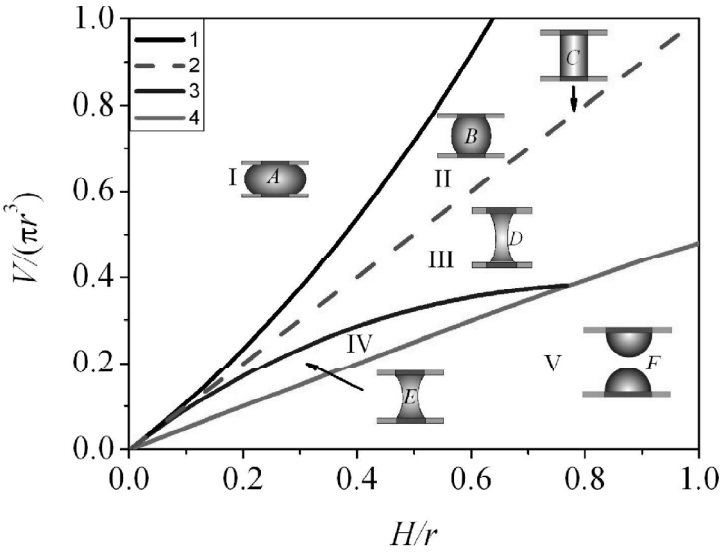

Figure 4: Phase Diagram for Different Morphologies of a Liquid Bridge

$$\left(\frac{\mathrm{d}\tilde{R}}{\mathrm{d}\tilde{H}}\right)_{\text{out}} = \frac{\left(2-\frac{\tilde{H}^2}{2}\right)\sqrt{4\tilde{R}^2-\tilde{H}^2}+\frac{\tilde{H}\tilde{R}^2}{2}\arcsin\frac{\tilde{H}}{2\tilde{R}}+\frac{\tilde{H}^2}{2}}{\left(6\tilde{R}^3-\tilde{R}\tilde{H}^2\right)\arcsin\frac{\tilde{H}}{2\tilde{R}}+2\tilde{H}\tilde{R}-\left(6\tilde{R}\tilde{H}+8\tilde{R}\arcsin\frac{\tilde{H}}{2\tilde{R}}\right)\sqrt{4\tilde{R}^2-\tilde{H}^2}}, \tag{22}$$

$$\left(\frac{\mathrm{d}\tilde{R}}{\mathrm{d}\tilde{H}}\right)_{\text{int}} = \frac{\left(2-\frac{\tilde{H}^2}{2}\right)\sqrt{4\tilde{R}^2-\tilde{H}^2}+\frac{\tilde{H}\tilde{R}^2}{2}\arcsin\frac{\tilde{H}}{2\tilde{R}}-\frac{\tilde{H}^2}{2}}{\left(6\tilde{R}^3-\tilde{R}\tilde{H}^2\right)\arcsin\frac{\tilde{H}}{2\tilde{R}}-2\tilde{H}\tilde{R}+\left(8\tilde{R}\arcsin\frac{\tilde{H}}{2\tilde{R}}-6\tilde{R}\tilde{H}\right)\sqrt{4\tilde{R}^2-\tilde{H}^2}} \tag{23}$$

for the cases of out-bulging ($0.638 \le \tilde{H} < 1$) and in-curving ($1 < \tilde{H} \le 3.485$), respectively. Substituting Eqs. (22) and (23) into (21), the liquid bridge forces for an out-bulging ($0.638 \le \tilde{H} < 1$) and an in-curving ($1 < \tilde{H} \le 3.485$) liquid bridge are respectively derived as

$$f_{\text{out}} = \frac{2}{\sqrt{4\tilde{R}^2 - \tilde{H}^2}} \left\{ \frac{\mathrm{d}\tilde{R}}{\mathrm{d}\tilde{H}} \left[8\tilde{R}^2 \arcsin\left(\frac{1}{2}\tilde{H}/\tilde{R}\right) - 2\tilde{H}\sqrt{4\tilde{R}^2 - \tilde{H}^2} + 2\tilde{H} \right.\right. \tag{24}$$

$$\left.\left. -2\arcsin\left(\frac{1}{2}\tilde{H}/\tilde{R}\right)\left(\sqrt{4\tilde{R}^2 - \tilde{H}^2} + \tilde{H}^2/4\right)\right] - \tilde{R}\tilde{H}\arcsin\left(\frac{1}{2}\tilde{H}/\tilde{R}\right) - 2\tilde{R} \right\}$$

$$f_{\text{in}} = \frac{2}{\sqrt{4\tilde{R}^2 - \tilde{H}^2}} \left\{ \frac{\mathrm{d}\tilde{R}}{\mathrm{d}\tilde{H}} \left[-8\tilde{R}^2 \arcsin\left(\frac{1}{2}\tilde{H}/\tilde{R}\right) + 2\tilde{H}\sqrt{4\tilde{R}^2 - \tilde{H}^2} + 2\tilde{H} \right.\right.$$

$$\left.\left. -2\arcsin\left(\frac{1}{2}\tilde{H}/\tilde{R}\right)\left(\sqrt{4\tilde{R}^2 - \tilde{H}^2} - \tilde{H}^2/4\right)\right] + \tilde{R}\tilde{H}\arcsin\left(\frac{1}{2}\tilde{H}/\tilde{R}\right) - 2\tilde{R} \right\} \tag{25}$$

The liquid bridge force calculated from Eqs. (4), (6) and (22–25) is plotted as a function of $\tilde{H}$ in Fig. 6, where $\tilde{V} = 1$. In the range of $0.638 \le \tilde{H} < 1$, the liquid bridge bulges out, and its liquid bridge force may be repulsive ($f > 0$) for a smaller $\tilde{H}$ and attractive ($f < 0$) for a larger $\tilde{H}$. There exists a certain volume of $\tilde{H}$ at which the free energy has a minimum and the liquid bridge force $f = 0$.

In the range of $0.638 \le \tilde{H} < 1$, however, the force f always brings the system into the configuration for which the bridge has the minimum free energy, and the liquid bridge possesses a preferred contact angle in the range of $\pi/2 < \theta < \pi = \theta_D$. However, in the range of $1 < \tilde{H} \le 3.485$, the liquid bridge always brings on an attractive force to the plates, but the force isn't a monotonous function about $\tilde{H}$.

The above results can be easily understood from the origins of the liquid bridge. In fact, the bridge force is composed mainly of two parts:

$$f = f_{\text{ST}} + f_{\text{Lap}}, \tag{26}$$

where f_{ST} and f_{Lap} denote the liquid force induced by surface tension and Laplace pressure difference, respectively. f_{ST} in the right side of Eq. (26) is always negative because the surface tension always attracts the two plates. However, f_{Lap} may be positive or negative, depending on the sign of Δp or the liquid bridge shape. If $\Delta p < 0$, the Laplace pressure difference of the out-bulging configuration produce a repulsive force to the plates, so the resultant

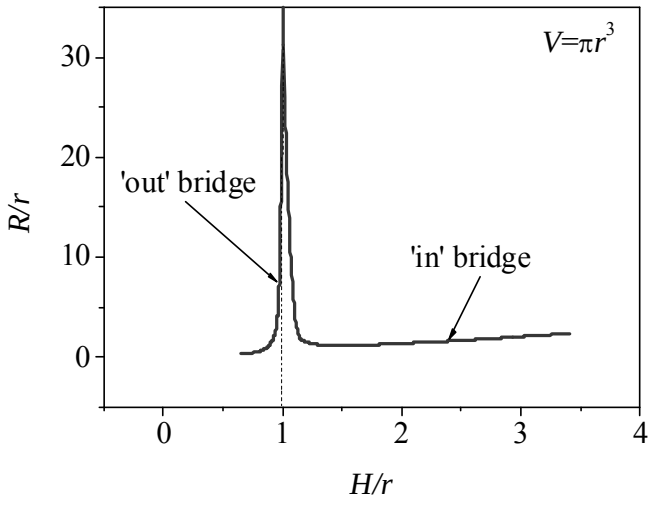

Figure 5: The Dependence Relationship of the Curvature Radius of a Liquid Bridge upon the Spacing of the Two Plates, where $\tilde{V} = 1.0$

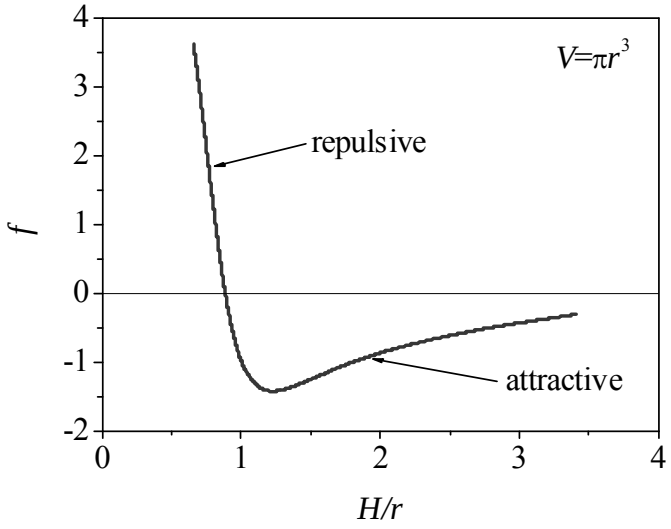

Figure 6: The Liquid Bridge Force, where $\tilde{V} = 1.0$

force f may be positive (repulsive) or negative (attractive). But $\Delta p > 0$, the force f_{Lap} provided by Laplace pressure difference is also negative, so the resultant force f is invariably negative.

4. CONCLUSIONS

In summary, we have presented a three-dimensional model to investigate the morphological transition phenomenon of a liquid bridge confined between two plates and to calculate the liquid bridge force. The two plate substrates are flat, parallel, and hydrophobic, each of which contains circular and hydrophilic surface domains. It is shown that six different morphologies of the wetting phase are possible dependent upon the Laplace pressure difference and the separation of the two plates. The diagram for these different morphologies of the liquid bridge is given, allowing us to determine the liquid bridge shape from its volume and height. In particular, a liquid bridge spanning between two solid surfaces causes a force acting on the two plates. The liquid bridge force can be attractive or repulsive and vanishes at a special spacing of the two plates. The bridge state induces an effective interaction between the two substrates, and the expression of the liquid bridge force is derived. The obtained results might be helpful for a better understanding of some wetting phenomena for industry to biology and can be used to estimate the influence of liquid bridge forces (or capillary forces) in microsized devices and systems. It is also mentioned that the present model can be extended easily to analyze some other configurations of liquid bridges.

Acknowledgement

This project was supported by the National Natural Science Foundation of China under Grant No 10802099 and Doctoral Fund of Ministry of Education of China under Grant No 200804251520.

References

[1] Lipowsky, R., Lenz, P. and Swain, P. S., "Wetting and Dewetting of Structured and Imprinted Surfaces," *Colloid. Surface. A*, **161**, 3–22, (2000).

[2] Zheng, Q. S., Yu, Y. and Zhao, Z. H., "Effects of Hydraulic Pressure on the Stability and Transition of Wetting Modes of Superhydrophobic Surfaces," *Langmuir*, **21**, 12207–12212, (2005).

[3] Hosono, E., Fujihara, S., Honma, I. and Zhou, H., "Superhydrophobic Perpendicular Nano-pin Film by the Bottom-up Process," *J. Amer. Chem. Soc.*, **127**, 13458–13459, (2005).

[4] Onda, T., Shibuichi, S., Satoh, N. and Tsujii, K., "Supper-water-repellent Fractal Surfaces," *Langmuir*, **12**, 2125–2127, (1996).

[5] Lenz, P. and Lipowsky, R., "Morphological Transition of Wetting Layers on Structured Surfaces," *Phys. Rev. Lett.*, **80**, 1920–1923, (1998).

[6] Gau, H., Herminghaus, S., Lenz, P. and Lipowsky R., "Liquid Morphologies on Structured Surfaces: from Microchannels to Microchips," *Science*, **283**, 46–49, (1999).

[7] Lenz, P., Bechinger, C., Schafle, C., Leiderer P. and Lipowsky R., "Perforated Wetting Layers from Periodic Patterns of Lyophobic Surface Domains," *Langmuir*, **17**, 7814–7822, (2001).

[8] Lenz, P., Fenzl, W. and Lipowsky R., "Wetting of Ring-shaped Surface Domains," *Europhys. Lett.*, **53**, 618–624, (2001).

[9] Lipowsky, R., "Morphological Wetting Transitions at Chemically Structured Surfaces," *Curr. Opin. Colloid In.*, **6**, 40–48, (2001).

[10] Brinkmann, M. and Lipowsky, R., "Wetting Morphologies on Substrates with Striped Surface Domains," *J. Appl. Phys.*, **92**, 4296–4306, (2002).

[11] Brinkmann, M., Kierfeld, J. and Lipowsky, R., "Stability of Liquid Channels or Filaments in the Presence of Line Tension," *J. Phys.: Condens. Matter*, **17**, 2349–2364, (2005).

[12] Fortes, M. A., "Axisymmetric Liquid Bridges between Parallel Plates," *J. Colloid Interf. Sci.*, **88**, 338–352, (1982).

[13] Fortes, M. A., Rosa, M. E., Vaz, M. F. and Teixeirap, P. I. C., "Mechanical Instabilities of Bubble Culusters between Parallel Walls," *Eur. Phys. J. E*, **15**, 395–406, (2004).

[14] Paddy, J. F., Petre, G., Rusu, C. G., Gamero, J. and Wozniak G., "The Shape Stability and Breakage of Pendant Liquid Bridges," *J. Fluid Mech.*, **352**, 177–204, (1997).

[15] Attard, P., "Thermodynamic Analysis of Bridging Bubbles and a Quantitative Comparison with the Measured Hydrophobic Attraction," *Langmuir*, **16**, 4455–4466, (2000).

[16] Makhovskaya, Y. Y. and Goryacheva, I. G., "The Combined Effect of Capillarity and Elasticity in Contact Interaction," *Tribol. Int.*, **32**, 507–515, (1999).

[17] Chen, Z. R. and Yu, S. W., "Capillary Adhesive Contact between a Spherical Rigid Punch and a Piezoelectric Half Space," *J. Appl. Phys.*, **94**, 6899–6907, (2003).

[18] Meseguer, J., Slobozhanin, L. A. and Perales J. M., "A Review on the Stability of Liquid Bridges," *Adv. Space Res.*, **16**, 5–14 (1995).

[19] Obata, K. J., Motokada, T., Saito S. and Takahashi K., "A Scheme for Micro-manipulation Based on Capillary Force," *J. Fluid Mech.*, **498**, 113–121, (2004).

[20] Qian, J. and Gao, H. J., "Scaling Effects of Wet Adhesion in Biological Attachment Systems," *Acta Biomater.*, **2**, 51–58, (2006).

[21] Sacquin, S. and Schoen, M., "Fluid Phase Transitions at Chemically Heterogeneous, Nonplanar Solid Substrates : Surface Versus Confinement Effects," *J. Chem. Phys.*, **118**, 1453–1465, (2003).

[22] Alencar, A. M., Wolfe, E. and Buldyrev, S. V., "Monte Carlo Simulation of Liquid Bridge Rupture: Application to Lung Physiology," *Phys Rev E.*, 026311, (2006).

[23] Swain, P. S. and Lipowsky, R., "Wetting between Structured Surfaces: Liquid Bridges and Induced Forces," *Europhys. Lett.*, **49**, 203–209, (2000).

[24] Valencia, A., Brinkmann, M. and Lipowsky, R., "Liquid Bridges in Chemically Structured Slit Pores," *Langmuir*, **17**, 3390–3399, (2001).

[25] Tas, N., Sonnenberg, T., Jansen, H., Letenberg, R. and Elwenspoek, M., "Stiction in Surface Micromachining," *J. Micromech. Microeng.*, **6**, 385–397, (1996).

[26] Wu, D., Fang, N., Sun, C. and Zhang, X., "Stiction Problems in Releasing of 3D Microstructures and its Solution," *Sensor. Actuat. A: Phys.*, **5**, 452–456, (2006).

[27] Ishikawa, M., Yoshimura, M., Ueda, K., "A Study of Friction by Carbon Nanotube Tip," *Appl. Surf. Sci.*, **188**, 456-459, (2002).

[28] Belaubre, P., Guirardel, M., Leberre, V., Pourciel, J. B., Bergaud C., "Cantilever-based Microsystem for Contact and Non-contact Deposition of Picoliter Biological Samples," *Sensor. Actuat. A: Phys.*, **110**, 130–135, (2004).

[29] Johnstone, R. W. and Parameswaran, M., "Theroretical Limits on the Freestanding Length of Cantilevers Produced by Surface Micromachining Technology," *J. Micromech. Microeng.*, **12**, 855–861, (2002).